BULLETIN OF THE POLISH ACADEMY OF SCIENCES
TECHNICAL SCIENCES, Vol. 74(1), 2026, Article number: e156768
DOI: 10.24425/bpasts.2025.156768

Production of environmentally friendly, sustainable insulation material: Fly ash-based geopolymer

Evren ARIOZ*

Department of Chemical Engineering, Faculty of Engineering, Eskisehir Technical University, 26555, Turkey

Abstract. Geopolymer foams are sustainable, environmentally friendly, and low-cost materials. In this research, fly ash-based geopolymer foams were synthesized using a mixture of sodium hydroxide, sodium silicate, and hydrogen peroxide as the foaming agent. At a constant 80°C curing temperature, curing periods were varied to 4, 15, and 24 hours, while hydrogen peroxide ratios were varied to 0.5%, 1%, 1.5%, and 2%. The effects of peroxide amount and curing duration on thermal conductivity, density, compressive strength, and microstructural properties were examined. The densities and thermal conductivity values decreased with increasing curing duration and hydrogen peroxide ratio. The lowest density was recorded as 1070 kg/m^3 for the sample prepared with 2% hydrogen peroxide and cured for 24 hours. Conductivity values varied from 0.247 to 0.108 W/m K. The highest compressive strength value obtained was 9.3 MPa. Quartz and mullite were identified as crystalline phases. The hydrogen peroxide content did not significantly affect the crystalline structures. The weight loss decreased as the hydrogen peroxide ratio increased, according to TGA analysis. BET analysis indicated that the pore size distribution shifted to the smaller pore size region as the peroxide concentration increased. SEM analyses showed a reduction in the presence of unreacted fly ash residues in the samples containing 1.5% and 2% hydrogen peroxide. The geopolymer foams produced in this experimental study meet RILEM requirements for structural and insulating concrete materials with respect to thermal conductivity and compressive strength.

Keywords: geopolymer; fly ash; foam; thermal conductivity; microstructure.

1. INTRODUCTION

Globally, CO_2 concentration increased by approximately 150%, reaching 413.2 parts per million (ppm) in 2020. As a result, governments were called upon to minimize carbon dioxide (CO_2) emissions with the Paris Agreement. The use of energy for residential purposes represents a major contributor to CO_2 emissions and is growing because of urbanization, particularly in emerging countries. The building industry is one of the primary sectors in cities that generates the most CO_2 emissions [1]. In fact, the construction industry accounts for around 40% of all energy and carbon dioxide emissions in developed countries [2].

In recent years, developments in the construction sector have increased interest in cost-effective and sustainable materials and encouraged the development of innovative building materials. As awareness of urban pollution and sustainable development increases, energy-efficient buildings that provide thermal insulation have also begun to attract attention [3]. For the building materials industry, the production and development of eco-friendly and low-cost insulation materials is of immense importance.

The current approach of the construction sector towards a sustainable environment is inadequate in terms of ecological protection. In recent years, due to the increasing awareness of global pollution and resource depletion, many researchers have focused on the use of waste materials in concrete. Geopolymers are one of the most promising alternatives due to their ability to be produced from waste materials. Geopolymers can be synthesized from various natural materials or industrial byproducts, such as slag and fly ash [4, 5]. Fly ash is quite remarkable among the source materials of geopolymers owing to its fine particle size. Fly ash is a residue found in the flue gases from the combustion of coal in thermal power plants and is collected from electrostatic precipitators. All around the world, fly ash is produced at approximately 500 million tons annually, and about 25% is utilized in construction areas. In addition to geopolymers, fly ash can also be used to produce zeolites by hydrothermal synthesis with sodium or potassium alkali solutions and as a low-cost adsorbent in wastewater treatment. The rest is disposed of in landfills at high costs and creates serious environmental problems [6]. Therefore, there is a need for solutions for safe waste disposal and the search for alternative materials that reduce environmental impacts. Geopolymers have gained renewed attention as sustainable alternatives to reduce CO_2 emissions and, therefore, global warming and waste disposal.

Geopolymers, which are classified as inorganic polymers, are produced by activating aluminosilicate-based materials with silicate solutions in an alkaline environment. The geopolymerization reactions start with the dissolution of precursors from the raw material into solution, continue with the coagulation and gelation of dissolved species, and end with polymerization. The process begins with hydrolysis by replacing H^+ on the solid surface with K^+ or Na^+ cations in the bulk solution. In a highly alkaline medium, Si-O-Si or Al-O-Al bonds in raw material break down and create $Si(OH)_4$ and $Al(OH)_4^-$ oligomers in the solution. Tetrahedral silicate and aluminate species reorganize and join in a three-dimensional network to form amorphous

*e-mail: evrenbayram@eskisehir.edu.tr

Manuscript submitted 2025-03-21, revised 2025-10-07, initially accepted for publication 2025-10-08, published in January 2026.

geopolymers. Alkali cations balance the negative charges related to the tetrahedral Al(III) unit [4,7,8].

Geopolymer foams are promising materials among other materials in the building industry. Foam concrete is typically known as lightweight concrete that can be produced with or without aggregate, containing a high degree of voids [4]. The air voids inside the materials reduce heat transfer, thus allowing the production of both heat and sound insulation materials. Foamed geopolymers have significant advantages compared to other insulation materials or foamed ceramics due to their low synthesis temperatures. Geopolymer foams are value-added materials that also offer fire-retardant properties in addition to insulation [8,9].

Geopolymer foams can be produced by two main methods: pre-foaming and mixed-foaming procedures. When compared to the pre-mixing method, the mixed-foaming procedure provides geopolymers with increased porosity, reduced thermal conductivity, and lower density [10]. The densities of geopolymer foams vary between 300 and 1800 kg/m^3, while the density of ordinary concrete ranges between 2200 and 2600 kg/m^3 [11]. The thermal conductivity and compressive strength values of geopolymer foams are in the range of 0.07–0.4 W/m K and 0.2–21 MPa, respectively [8].

The most common synthesis method of geopolymer foams is the addition of chemicals such as hydrogen peroxide to the geopolymer paste. Foams can also be produced using organic foaming agents such as detergents and resin soap, which introduce enormous amounts of air bubbles into the mixture. Hydrogen peroxide is the most used foaming agent, which easily decomposes into H_2O and O_2 in alkaline solutions and creates controlled air bubbles in geopolymer slurry [8,12]. In this study, fly ash-based geopolymer foams were produced by alkali activation of fly ash using hydrogen peroxide as a foaming agent to develop insulation and construction materials that meet international standards. The effects of the hydrogen peroxide ratio on the physical and structural properties of foams were investigated. The effects of the resulting porosity on thermal conductivity and density values, which are critical for insulation materials, and on compressive strength values, which are critical for building materials, were investigated.

2. MATERIALS AND METHODS

2.1. Geopolymer foam production

Geopolymer foams were produced by activation of fly ash with sodium hydroxide and sodium silicate, and using hydrogen peroxide as a foaming agent. The chemical composition of the fly ash supplied by Catalagzi Thermal Power Plant in Turkey, analyzed by X-ray fluorescence spectrometry (Rigaku ZSX Primus), is given in Table 1. The results revealed that the fly ash used in the experiments is adequate for the prescribed chemical composition according to the ASTM C 618 standard for coal fly ashes.

The phase analysis of fly ash is given in Fig. 1. The XRD pattern of the raw fly ash showed a dominant quartz and mullite crystalline structure with sharp and intense peaks. The hump observed between 18–38° 2θ in the XRD pattern indicates the

Table 1
Chemical composition of fly ash used in geopolymer synthesis

Composition	%
SiO_2	57.2
Al_2O_3	25.1
Fe_2O_3	7.3
CaO	1.7
MgO	1.8
SO_3	0.2
Na_2O	0.4
K_2O	4.8
LOI*	1.6

LOI* = Loss on ignition

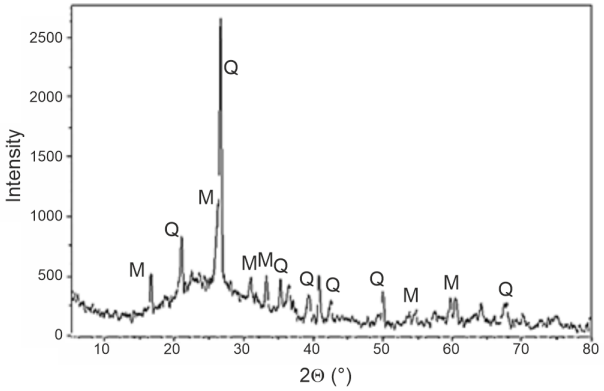

Fig. 1. XRD pattern of fly ash

presence of an amorphous phase, and thus, the fly ash is suitable for geopolymerization reactions.

The FTIR spectrum of fly ash is given in Fig. 2. The major peaks observed at 1075 cm^{-1} and 1100 cm^{-1} are linked to the asymmetric stretching vibrations of Si-O(Si, Al), while the bending vibrations of O-Si-O are observed at 458 cm^{-1} [13]. The peak seen at 2900 cm^{-1} is attributed to asymmetric stretching vibrations of -CH_2- [14]. The bending vibrations of the -OH

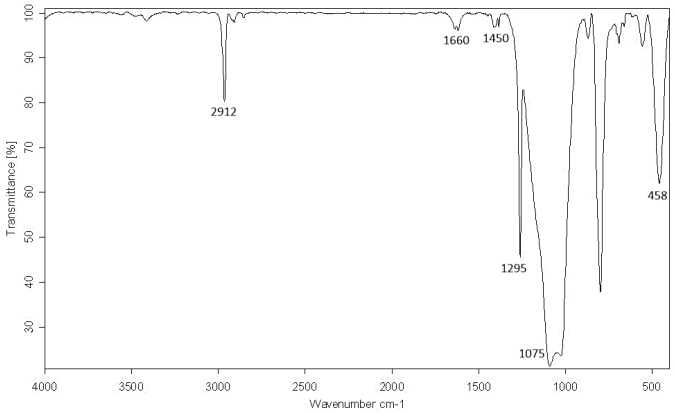

Fig. 2. FTIR spectrum of fly ash

group are observed at 1660 cm^{-1}. The peak at 1450 cm^{-1} corresponds to C-O stretching vibrations [13]. The peak at 1295 cm^{-1} is assigned to asymmetric bending vibrations [15]. The peaks observed between 800–600 cm^{-1} are assigned to the symmetric stretching and bending vibrations of Si-O-Si(Al), which indicate the presence of aluminosilicates [13].

Fly ash was activated by technical grades of sodium hydroxide and sodium silicate solutions. Sodium hydroxide was prepared at a concentration of 12 M. Sodium silicate was added to the sodium hydroxide solution at a weight ratio of 1:1 to obtain an alkali activator solution, which was added to fly ash at a weight ratio of 0.4. Technical grade hydrogen peroxide of 50% was used as a foaming agent. The density and pH value of hydrogen peroxide were 1.19 g/cm^3 and 4.5, respectively. Hydrogen peroxide was added to the homogeneous geopolymer paste at 0.5%, 1%, 1.5% and 2% by weight to investigate whether geopolymer foam could be synthesized at low dosages. The foamed pastes were poured into three-gang steel molds ($40 \times 40 \times 160$ mm) in compliance with EN 196-1. The geopolymer foams were cured at a temperature of 80°C for 4, 15, and 24 hours in a laboratory oven and then aged for 7 and 28 days under atmospheric conditions.

2.2. Geopolymer characterization

The apparent density, thermal conductivity, and compressive strength of the foams were determined at the age of 28 days. The density values were determined by measuring the weight of dry foamed samples and dividing by their volume [12]. The specific strength values were obtained by dividing compressive strength values by density [9]. Thermal conductivity values were determined by the Mathis TCi Thermal Property Analyzer at room temperature. The compressive strength tests were conducted on all geopolymer specimens after 7 and 28 days of aging at a loading capacity of 2400 ± 200 N/s. Density and thermal conductivity values were measured using each prism specimen, and the average of three measurements was calculated and recorded. The compressive strength values for the 7-day and 28-day aged specimens given in the figures represent the average of six separate measurements. The strength tests were performed on samples aged for 7 and 28 days to enable comparison with existing standards and requirements used for traditional cementitious materials.

Microstructures were investigated by using the specimens cured for 24 hours and aged for 28 days. The crystalline phases were identified by X-ray diffractometer (Rigaku Rint 2000, Japan) with Cu-Kα (1.54 A°) radiation (30 mA–40 kV) at the 2θ detection range between 5°–80°. The identification of functional groups was carried out using Fourier transform infrared spectroscopy (FTIR) with 64 scans and 2 cm^{-1} of resolution between 400 and 4000 cm^{-1} with a KBr pellet. The morphologies of the geopolymer foams were analyzed by scanning electron microscope (SEM) (Zeiss Evo 50 EP) with 20 kV accelerating voltage. Each sample used in the SEM analysis was kept under vacuum to remove any remaining contamination. Thermal stabilities were determined by a thermogravimetric analyzer (TGA) under a nitrogen atmosphere at 30°C to 850°C with a 10°C/min heating rate. The pore size distribution was characterized by a N_2 adsorption-desorption analyzer using a Quantachrome TouchWin device. The samples were degassed at 120°C for 12h under a nitrogen atmosphere. The Barret-Joyner-Halenda (BJH) method was applied to determine the pore diameter distribution.

3. RESULTS AND DISCUSSION

3.1. Density

The apparent densities of the geopolymer foams aged for 28 days are given in Fig. 3. Test results showed that the densities of the geopolymer foams decreased both with an increase in curing duration and an increase in hydrogen peroxide ratio. For example, the densities of the samples cured for 4 hours were found to be 1480 kg/m^3 and 1250 kg/m^3 for hydrogen peroxide contents of 0.5% and 2%, respectively. This can be attributed to the higher porosity obtained at higher hydrogen peroxide ratios. When the curing duration increased from 4 hours to 24 hours, the density of geopolymer foams produced with 2% hydrogen peroxide decreased from 1250 kg/m^3 to 1070 kg/m^3. This can be attributed to the evaporation of water that may be present in the geopolymer foam as time increases.

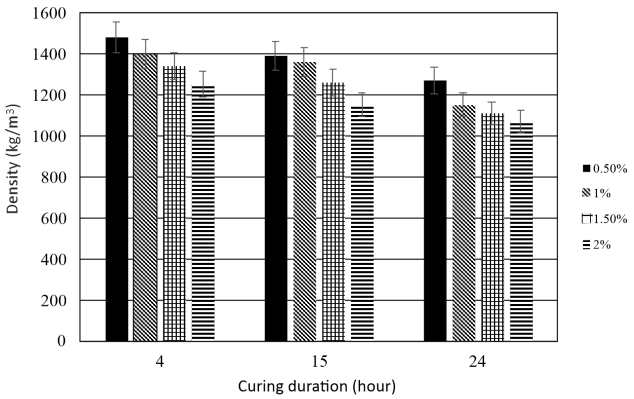

Fig. 3. Densities of geopolymer foams

The highest density was obtained as 1480 kg/m^3 for the foam prepared with 0.5% hydrogen peroxide and cured for four hours, while the lowest density was obtained as 1070 kg/m^3 for the sample prepared with 2% hydrogen peroxide and cured for 24 hours. The densities of geopolymer foams produced by different researchers were found to be between 715 and 1700 kg/m^3 [2, 11].

3.2. Thermal conductivity

The thermal conductivity values of the geopolymer foams are given in Fig. 4. The average of three measurements for each sample was recorded.

Test results indicated that thermal conductivity values were reduced both by increasing curing duration and hydrogen peroxide content. For example, the thermal conductivity values for the samples prepared with 1% hydrogen peroxide were recorded as 0.245 and 0.121 W/m K for the curing durations of 4 and 24 hours, respectively. In other words, when the curing duration

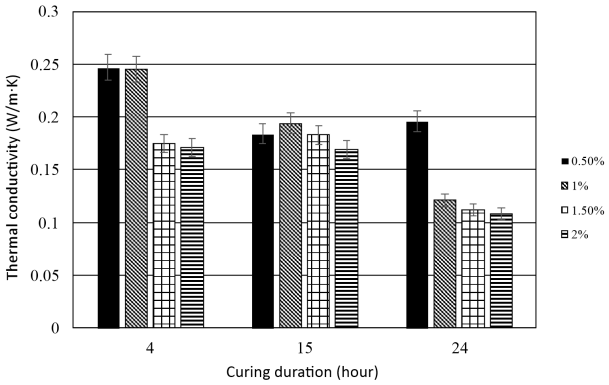

Fig. 4. The thermal conductivity values of geopolymer foams

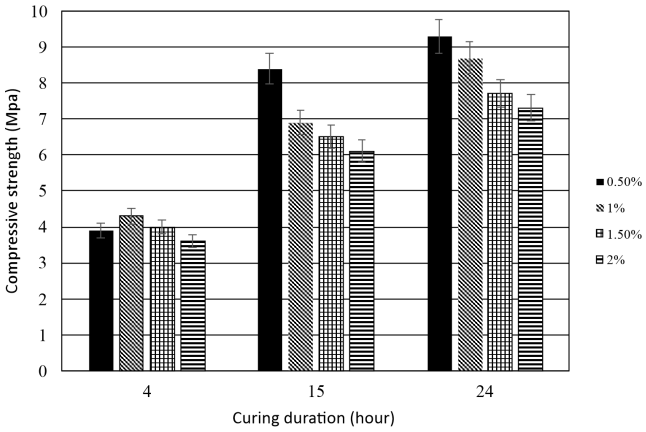

Fig. 6. The compressive strength values of geopolymer foams aged for 28 days

increased from 4 hours to 24 hours, the thermal conductivity decreased by 50%. The highest and the lowest conductivity values were obtained as 0.247 W/m K and 0.108 W/m K for the samples produced with 0.5% hydrogen peroxide and cured for 4 hours and 2% hydrogen peroxide and cured for 24 hours, respectively. The lower conductivity values were attributed to the higher amounts of void, including air, which is a poor thermal conductor. In addition, the fact that the measured thermal conductivity values do not fit into a pattern that can be formulated is an indication that the pores in the foams were not evenly distributed.

3.3. Compressive strength

The compressive strengths of geopolymer foams aged for 7 and 28 days are given in Fig. 5 and Fig. 6, respectively. Test results revealed that the compressive strength of the geopolymer foams decreased with an increase in hydrogen peroxide content and increased with the growth of curing duration. For example, compressive strength values of the specimens cured for 24 hours and then aged for 7 days were determined as 8.5 MPa and 7.1 MPa for 0.5% and 2% hydrogen peroxide contents, respectively. The compressive strength values rose from 3.8 MPa to 8.5 MPa when the curing duration increased from 4 hours to 24 hours for the specimens produced with 0.5% hydrogen peroxide content. The positive effect of curing duration on the compressive strength values was attributed to the enhanced geopolymer gel formation with longer curing, resulting in a stronger bond.

The compressive strength development of the geopolymer foams aged for 28 days was similar to that of the geopolymer foams aged for 7 days. The highest compressive strength was found to be 9.3 MPa, obtained for the sample prepared with a 0.5% hydrogen peroxide ratio, cured for 24 hours, and aged for 28 days. It should be noted that the strength values slightly increased with an increase in the aging of the samples.

The specific strengths of the geopolymer foams calculated by dividing compressive strength by density are given in Fig. 7. The specific strength values varied between 2635 N m/kg and 7565 N m/kg. The specific strengths of geopolymer foams increased with increasing curing duration applied to the samples. For example, while the specific strengths of the samples cured for 4 hours were at the level of 3000 N m/kg, the specific strengths of the samples that were cured for 24 hours reached the levels of 7000 N m/kg. The findings showed that the change in the specific strength values was compatible with the changes in the compressive strength and density values. Moreover, the results indicated that foams have high compressive strength even at low density.

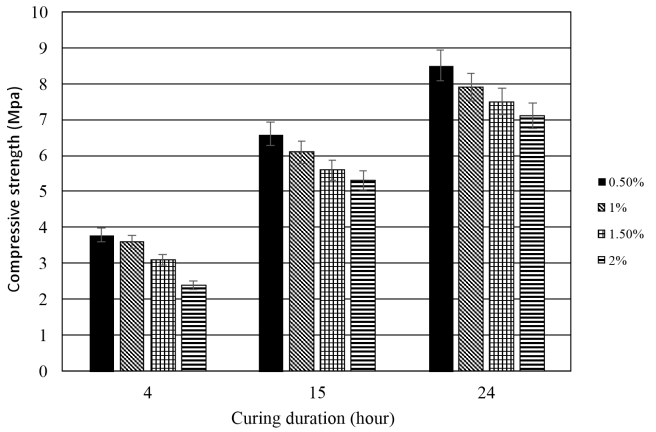

Fig. 5. The compressive strength values of geopolymer foams aged for 7 days

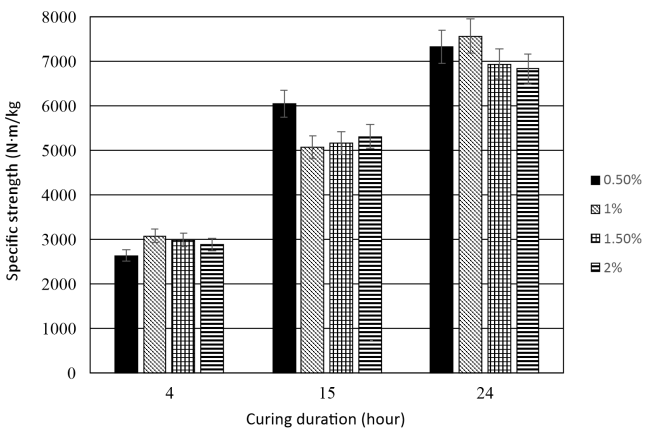

Fig. 7. The specific strengths of geopolymer foams aged for 28 days

3.4. Characterization of foams

3.4.1. X-ray diffractometry (XRD) analysis

The crystalline structures of the geopolymer foams were determined by X-ray diffractometry, and the patterns are presented in Fig. 8. The characteristic halo indicating amorphous structure seen in the diffractogram of fly ash was not observed in the patterns of geopolymer foams; instead, a small, uncertain rise was seen for all the foam samples. The peak intensity of the amorphous structure was too weak to be distinguished from the pattern background, so a specific halo could not be observed.

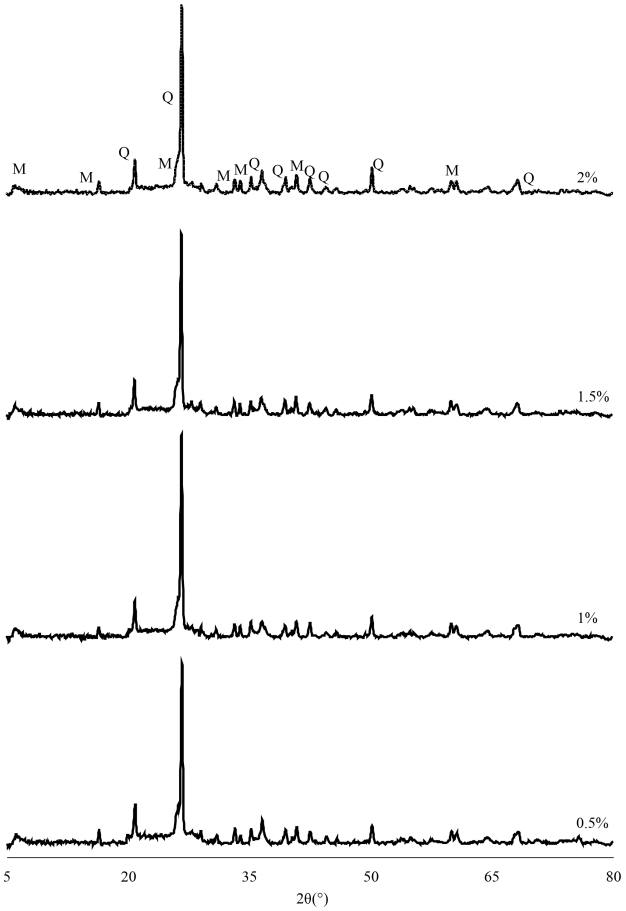

Fig. 8. XRD patterns of geopolymer foams

The main crystalline phases observed in the foam samples were quartz and mullite. Since Si and Al are in the structure of fly ash, quartz and mullite crystals originate from insoluble fly ash particles. These peaks also indicated that the fly ash particles were not completely dissolved in the medium. Since the strong bond structure of quartz is difficult to break, the crystals cannot be included in the gel structure. The change in hydrogen peroxide content did not significantly affect the phase assemblage of the geopolymer foams.

3.4.2. Fourier transform infrared spectroscopy (FTIR) analysis

Fourier transform infrared spectroscopy (FTIR) bands of the foams are given in Fig. 9. The asymmetric stretching of Al-O and Si-O bonds originating from individual tetrahedra, which are the main fingerprints of the matrix, was observed at ~ 1000 cm^{-1} [16]. The intensities of the bands were decreased as the hydrogen peroxide ratio increased. The decrease in the intensity of FTIR absorption bands with increasing hydrogen peroxide content is attributed to the dissolution of these phases in an alkaline medium. The participation of aluminum and silica phases in the structure and the presence of nonbridging oxygen in the geopolymer gel phase caused a diminutive change in the wavelength of the peak [13]. The shift to higher wavelength also indicated the increasing silica content in the structure. The incorporation of Si_4^+ into the gel phase causes the T-O-T angle to decrease. The signal appears at a lower frequency due to the longer Al-O bond than the Si-O bond [17]. The band seen at 470 cm^{-1} can be assigned to the in-plane bending vibrations of Al-O and Si-O bonds [16]. The intensity of asymmetric stretching of Al-O and Si-O bonds decreased as the hydrogen peroxide content increased. It can be concluded that increasing the void amount hindered the formation of these bonds.

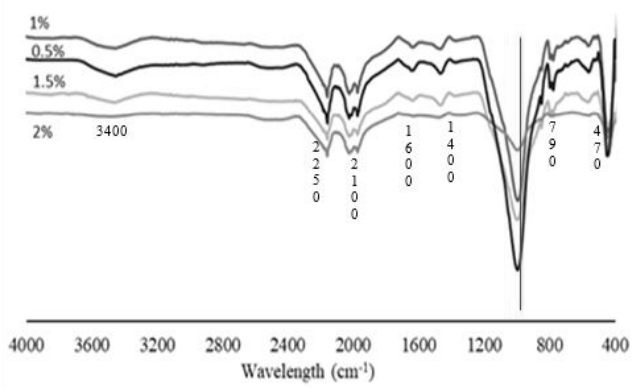

Fig. 9. FTIR spectra of geopolymer foams

FTIR analysis revealed structural changes in the raw fly ash. The sharp peaks observed in the structure of the fly ash were observed to be less dense and wider in the geopolymer foam structure. The formation of a new amorphous aluminosilicate network was determined through peak broadening and shifting, especially in the fingerprint region.

Strong Si-OH valence vibrations were seen in the region 2250–2100 cm^{-1} [18]. The double bands observed at 780 cm^{-1} and 790 cm^{-1} were attributed to quartz originating from fly ash [13]. The bands observed at 3400 cm^{-1} and 1600 cm^{-1} were attributed to O-H stretching and bending of water molecules, respectively, indicating weakly bound water molecules adsorbed on the surface or trapped in large pores [5]. The stretching vibrations of the C-O bond, indicating sodium carbonate formation, were observed at approximately 1400 cm^{-1} [13].

3.4.3. Scanning electron microscopy (SEM) analysis

The morphology and microstructure of the geopolymer foam samples were observed by scanning electron microscopy (SEM). Images at different magnifications obtained by SEM analyses are given in Fig. 10. The figure clearly shows the differences in the densities and morphologies of the foam samples. The foam samples exhibited heterogeneous structures with many pores of

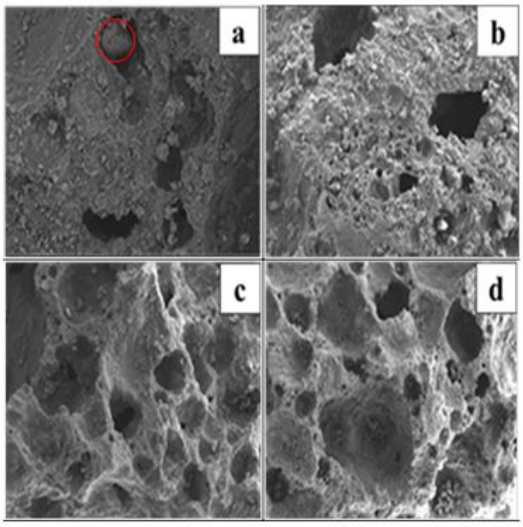

Fig. 10. SEM images of geopolymer foams with ×100 magnification: (a) 0.5%, (b) 1%, (c) 1.5%, (d) 2%

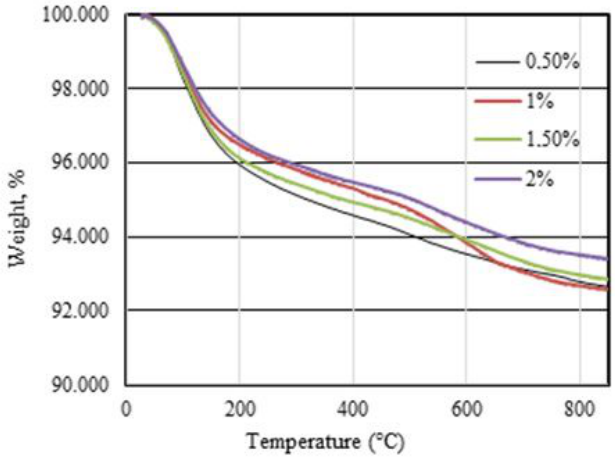

Fig. 11. Thermogravimetric curves of geopolymer foams

different diameters. As the hydrogen peroxide ratio increased, the structure of the samples became less compact.

SEM images revealed that some unreacted fly ash particles remained in the structure, especially in Fig. 10a and Fig. 10b. The number of unreacted particles decreased as the peroxide content in the mixture increased to 1.5% and 2%. With the increase in hydrogen peroxide content, the number of pores increased, while the diameter of the pores decreased. As the pore amount increased, the geopolymeric gel phase between the pores decreased, and thinner walls were formed, resulting in lower compressive strength values. While needle-shaped crystals of small size were seen in the images of the samples produced with 0.5% and 1% hydrogen peroxide, these crystals disappeared in the samples containing 1.5% and 2% peroxide.

3.4.4. Thermogravimetric analyses (TGA) – analysis

The thermogravimetric analysis (TGA) method serves as an extremely useful tool for understanding the thermal phenomena associated with polymer composites. TGA results of geopolymer foams cured for 24 hours and aged for 28 days are given in Fig. 11.

As can be seen from Fig. 11, the curves have similar variations up to 400°C. As the hydrogen peroxide ratio increased, weight loss decreased. The thermal behavior of geopolymer foams was analyzed in three zones: Zone I (up to 100°C), Zone II (between 100°C and 300°C), and Zone III (above 300°C). In Zone I, the water adsorbed on the surface and in the large pores evaporated to form foam samples. The weight loss between 100°C and 250°C can be attributed to chemically bound water in the small pores. The weight loss in Zone III is thought to be due to the removal of water in the form of silanol and aluminol groups by polycondensation of T–OH groups, where T represents Si or Al [19].

In TGA analysis, the mass loss in Region III is attributed to the polycondensation of silanol (Si–OH) and aluminol (Al–OH) groups in the geopolymer matrix, where T represents Si or Al. The presence of T–OH groups is typically indicated by broad absorption bands at 3400 cm^{-1} (O–H stretching vibrations) and around 1600 cm^{-1} (H–O–H bending vibrations). The Si–O and Al–O bands form the fingerprint region in the geopolymer matrix and are expressed by bands observed at cm^{-1} and 470 cm^{-1} wavelengths. The weight loss above 300°C for the sample synthesized with 2% hydrogen peroxide was less than the other foam samples. TGA analysis was consistent with the FTIR curves, and the intensity of the Si–O and Al–O stretching vibrations was the lowest in the same foam sample.

3.4.5. Brunauer-Emmett-Teller (BET) and Barrett-Joyner-Halenda (BJH) analysis

Brunauer-Emmett-Teller (BET) analysis provides precise pore size distribution data of powdered solids. N_2 adsorption-desorption isotherms and pore size distribution of the samples are given in Fig. 12 and Fig. 13. All synthesized samples exhibited a similar hysteresis loop at the same relative pressure; only the adsorbed volume decreased with increasing peroxide concentration. The N_2 adsorption-desorption isotherms indicated that the samples could be classified as Type IV isotherms according to IUPAC (International Union of Pure and Applied Chemistry) classifications defined for mesoporous adsorbents. These isotherms represent the H3 type hysteresis loop showing capillary condensation in mesopores [20].

The pore size distribution of the foams was determined by the Barrett-Joyner-Halenda (BJH) method. Geopolymer foams showed inhomogeneous pore size distribution as seen in Fig. 13. In the samples synthesized with 0.5% and 1% hydrogen peroxide, the geopolymer foams have mesopores concentrated between 8 nm and 20 nm. The pore size distribution shifted to the smaller pore size region as the peroxide concentration increased. Micropores of about 1.8 nm were also observed in other samples.

BJH analysis is also related to the compressive strength and thermal conductivity of geopolymer foams. The mesoporous structure observed in samples synthesized with 0.5% and 1% hydrogen peroxide results in slightly thicker pore walls, thus providing higher compressive strength. As the hydrogen peroxide

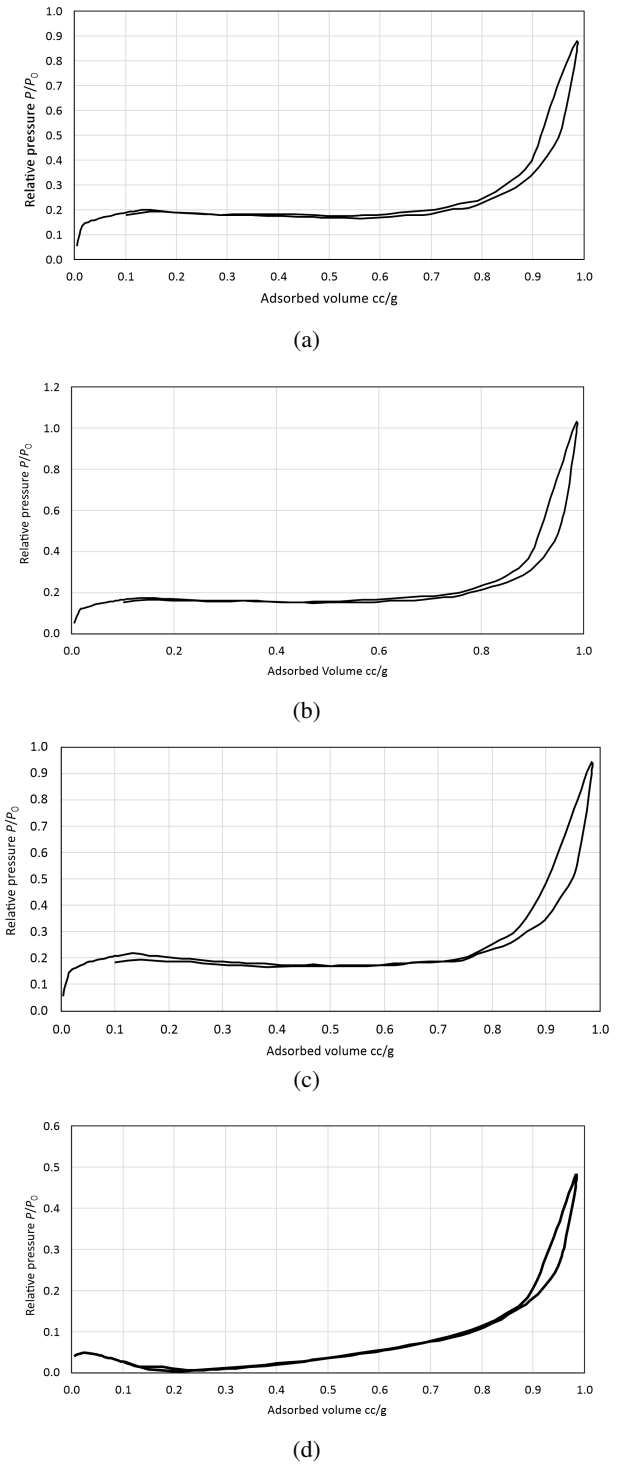

Fig. 12. N_2 isotherms of geopolymer foams produced with varying hydrogen peroxide amounts
(a) 0.5%, (b) 1%, (c) 1.5%, (d) 2%

content increases, BJH analysis shows a shift towards smaller pores. This increase in porosity weakens the framework and leads to thinner walls between the pores, resulting in a decrease in compressive strength. However, the increase in the number of smaller pores results in an increase in the number of air-filled voids, reducing heat transfer and thermal conductivity.

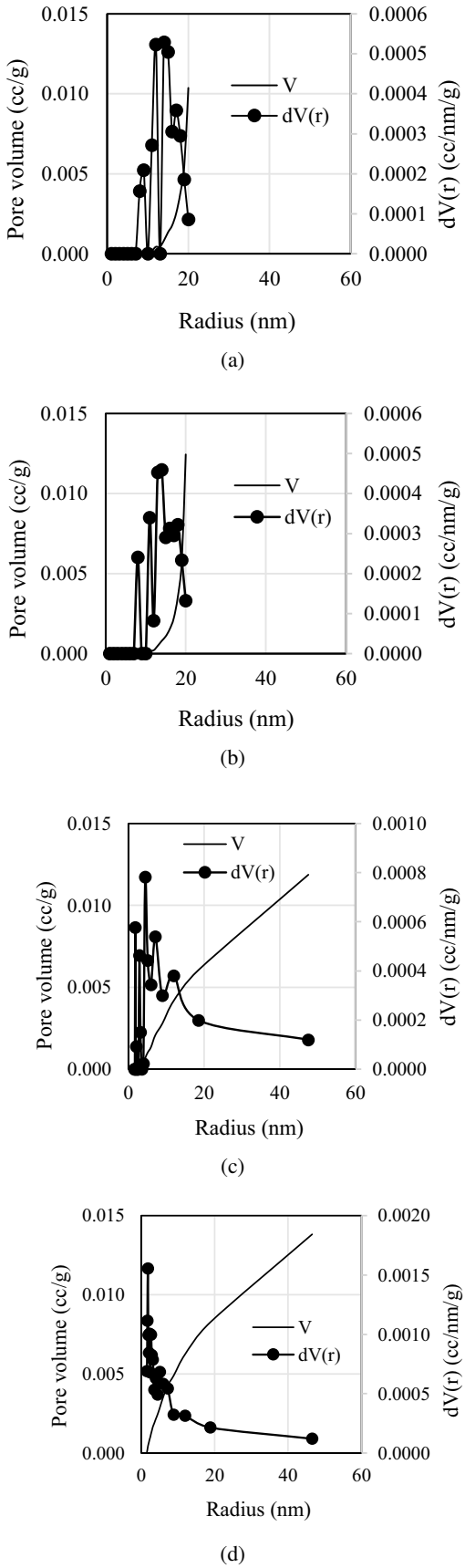

Fig. 13. Pore size distribution of the samples of geopolymer foams produced with varying hydrogen peroxide amounts
(a) 0.5%, (b) 1%, (c) 1.5%, (d) 2%

4. CONCLUSIONS

The results of the experiments conducted on the geopolymer foams produced in this experimental study can be summarized as follows. With the increase in the curing duration, the densities of the geopolymer foams decreased while their compressive strength increased. The increase in strength values can be attributed to stronger geopolymer bonds formed with longer curing durations. As the hydrogen peroxide content increased, density, thermal conductivity, and compressive strength values of the foams decreased. The specific strength values showed that the samples had high strength despite their low densities. The thermal conductivity of geopolymer foams decreased as both the curing duration and hydrogen peroxide content increased. Test results revealed that geopolymer foams have exceptionally low thermal conductivity values ranging from 0.247 W/m K to 0.108 W/m K. The phase assemblage of the foams did not change with the hydrogen peroxide content.

FTIR analysis showed that the disordered structure increased as the peroxide ratio increased. The increase in the amount of Si in the gel structure caused the Si-O main peak in the spectrum to shift to a higher wavelength. While the highest peak density was observed at 0.5% peroxide, the highest 28-day compressive strength was also measured in the same sample. It can be concluded that the Si bond was relatively less soluble as the peroxide ratio increased, and low amounts of hydrogen peroxide were insufficient to dissolve Si bonds. Unreacted fly ash particles were observed at a low hydrogen peroxide ratio, which was confirmed by SEM images.

SEM analysis indicated that higher peroxide ratios resulted in more but nonuniform pores in the structure. The increase in pore formation resulted in decreases in compressive strength values and a less dense structure. The images indicated the pores formed by the peroxide were heterogeneous, consistent with the BET analysis. BET analysis marked that the geopolymer foam synthesized with 2% peroxide also had micropores. As seen from SEM and confirmed by BET analysis, the pore diameters decreased as the hydrogen peroxide ratio increased. Geopolymer foams synthesized with different amounts of hydrogen peroxide had irregularly distributed pores of different diameters.

Compressive strength, FTIR, and SEM analysis results were found to be compatible with each other. The increase in the hydrogen peroxide ratio caused a less dense structure, a decrease in the strength of the bond, showing the fingerprint of the geopolymer matrix, and a decrease in the compressive strength. Thermogravimetric curves of geopolymer foams did not show significant changes. Thermogravimetry analyses demonstrated a gradual decrease as the temperature increased; degradation decreased as the hydrogen peroxide ratio increased.

Thanks to their relatively low thermal conductivity values, the geopolymer foams produced in this study can be an alternative to thermal insulation materials as a cost-effective and environmentally friendly material. According to RILEM (The International Union of Laboratories and Experts in Construction Materials), materials with a compressive strength between 3.5 and 15 MPa and a thermal conductivity of less than 0.75 W/m K. can be used for structural and insulating purposes [3]. It should be noted that most of the geopolymer foams produced in this experimental study meet these RILEM requirements for structural and insulating concrete materials in terms of thermal conductivity and compressive strength. In this study, thermal, structural, and microstructural properties of geopolymer foams were investigated. In future studies, it is planned to investigate their suitability for long-term applications in construction environments by investigating properties such as water absorption, freeze-thaw resistance, and chemical stability.

FUNDING

This study was financially supported by Eskisehir Technical University with Project No. 21GAP082 and Project No. 22ADP041.

REFERENCES

[1] L. Yu, S. Wu, L. Jiang, B. Ding, and X. Shi, "Do more efficient buildings lead to lower household energy consumption for cooling? Evidence from Guangzhou, China," *Energy Policy*, vol. 168, p. 113119, 2022, doi: 10.1016/j.enpol.2022.113119.

[2] Y.X. Chen, K.M. Klima, H.J.H. Brouwers, and Q. Yu, "Effect of silica aerogel on thermal insulation and acoustic absorption of geopolymer foam composites: The role of aerogel particle size," *Compos. B Eng.*, vol. 242, p. 110048, 2022, doi: 10.1016/j.compositesb.2022.110048.

[3] M.Y.J. Liu, U.J. Alengaram, M.Z. Jumaat, and H.K. Mo, "Evaluation of thermal conductivity, mechanical and transport properties of lightweight aggregate foamed geopolymer concrete," *Energy Build.*, vol. 72, pp. 238–245, 2014, doi: 10.1016/j.enbuild.2013.12.029.

[4] Z. Zhang, J.L. Provis, A. Reid, and H. Wang, "Geopolymer foam concrete: an emerging material for sustainable construction," *Constr. Build. Mater.*, vol. 56, pp. 113–127, 2014, doi: 10.1016/j.conbuildmat.2014.01.081.

[5] X. Zhao *et al.*, "Interfacial study of steel slag-red mud-based geopolymer concrete with cement concrete substrates: bond strength and crack evolution," *J. Build. Eng.*, vol. 113, p. 114083, 2025, doi: 10.1016/j.jobe.2025.114083.

[6] M. Ahmaruzzaman, "A review on the utilization of fly ash," *Prog. Energy Combust. Sci.*, vol. 36, no. 3, pp. 327–363, 2010, doi: 10.1016/j.pecs.2009.11.003.

[7] Sindhunata, J.S.J. van Deventer, G.C. Lukey, and H. Xu, "Effect of curing temperature and silicate concentration on fly-ash-based geopolymerization," *Ind. Eng. Chem. Res.*, vol. 45, no. 10, pp. 3559–3568, 2006, doi: 10.1021/ie051251p.

[8] S. Yan *et al.*, "Green synthesis of high porosity waste gangue microsphere/geopolymer composite foams via hydrogen peroxide modification," *J. Clean. Prod.*, vol. 227, pp. 483–494, 2019, doi: 10.1016/j.jclepro.2019.04.185.

[9] W. Feng, Y. Jin, D. Zheng, Y. Fang, Z. Dong, and H. Cui, "Study of triethanolamine on regulating early strength of fly ash-based chemically foamed geopolymer," *Cem. Concr. Res.*, vol. 162, p. 107005, 2022, doi: 10.1016/j.cemconres.2022.107005.

[10] H.S. Hassan, H.A. Abdel-Gawwad, S.R.V. García and I. Israde-Alantra, "Fabrication and characterization of thermally-insulating coconut ash-based geopolymer foam," *Waste Manag.*, vol. 80, pp. 235–240, 2018, doi: 10.1016/j.wasman.2018.09.022.

[11] M.M.A.B. Abdullah, K. Hussin, M. Bnhussain, K.N. Ismail, Z. Yahya and R.A. Razak, "Fly ash-based geopolymer lightweight

concrete using foaming agent," *Int. J. Mol. Sci.*, vol. 13, no. 6, pp. 7186–7198, 2012, doi: 10.3390/ijms13067186.

[12] V. Ducman and L. Korat, "Characterization of geopolymer fly-ash based foams obtained with the addition of Al powder or H2O2 as foaming agents," *Mater. Charact.*, vol. 113, pp. 207–213, 2016, doi: 10.1016/j.matchar.2016.01.019.

[13] P. Rożek, M. Król, and W. Mozgawa, "Spectroscopic studies of fly ash-based geopolymers," *Spectrochim. Acta A Mol. Biomol. Spectrosc.*, vol. 198, pp. 283–289, 2018, doi: 10.1016/j.saa.2018.03.034.

[14] R. Caban and A. Gnatowski, "Analysis of the Impact of Waste Fly Ash on Changes in the Structure and Thermal Properties of the Produced Recycled Materials Based on Polyethylene," *Materials*, vol. 17, no. 14, p. 3453, 2024, doi: 10.3390/ma17143453.

[15] Md. H. Islam, D. Law, Y. Patrisia, and C. Gunasekara, "Blended brown coal and Class F fly ash based geopolymer," *Case Stud. Constr. Mater.*, vol. 23, p. e05036, 2025, doi: 10.1016/j.cscm.2025.e05036.

[16] J.W. Phair and J.S.J. van Deventer, "Effect of the silicate activator pH on the microstructural characteristics of waste-based geopolymers," *Int. J. Miner. Process.*, vol. 66, no. 1–4, pp. 121–143, 2022, doi: 10.1016/S0301-7516(02)00013-3.

[17] Fernández-Jiménez and A. Palomo, "Mid-infrared spectroscopic studies of alkali-activated fly ash structure," *Microporous Mesoporous Mater.*, vol. 86, no. 1–3, pp. 207–214, 2005, doi: 10.1016/j.micromeso.2005.05.057.

[18] K.O. Bugaev, A.A. Zelenina, and V.A. Volodin, "Vibrational spectroscopy of chemical species in silicon and silicon-rich nitride thin films," *Int. J. Spectrosc.*, vol. 2012, p. 281851, 2012, doi: 10.1155/2012/281851.

[19] T. Kovářík *et al.*, "Cellular ceramic foam derived from potassium-based geopolymer composite: Thermal, mechanical and structural properties," *Mater. Des.*, vol. 198, p. 109355, 2021, doi: 10.1016/j.matdes.2020.109355.

[20] P. He, Z. Guo, X. Zhang, T. Wang, W. Zheng, and D. Liu, "Development of sulfhydryl grafted hierarchical porous geopolymer for highly effective removal of Pb(II) from water," *Sep. Purif. Technol.*, vol. 334, p. 125954, 2024, doi: 10.1016/j.seppur.2023.125954.